Hindawi
Journal of Chemistry
Volume 2024, Article ID 1358495, 8 pages
https://doi.org/10.1155/2024/1358495

Research Article

Characterization of Gold Nanoparticles Synthesized with *Zingiber zerumbet* Extracts

Wayne C. Liao,[1] Collin S. Liao,[2] Yu-Chen Lin,[3] and Ching-Yi Lien[3]

[1]*Department of Nursing, Chang Gung University of Science and Technology, Chiayi, Taiwan*
[2]*Department of Biotechnology and Bioindustry Sciences, National Cheng Kung University, Tainan, Taiwan*
[3]*Department of Applied Chemistry, National Chia-Yi University, Chiayi, Taiwan*

Correspondence should be addressed to Ching-Yi Lien; kelly@mail.ncyu.edu.tw

Received 31 August 2023; Revised 9 January 2024; Accepted 30 January 2024; Published 7 February 2024

Academic Editor: Jose M. G. Martinho

Gold nanoparticles have been used as drug carriers and imaging reagents. The plant extract-capped gold nanoparticles provide better properties than chemically synthesized gold nanoparticles. In this study, *Zingiber zerumbet* extract-mediated green production of gold nanoparticles (Z. *zerumbet*@Au NPs) was established. Based on the UV-visible spectroscopy and transmission electron microscope (TEM) results, most *Z. zerumbet*@Au NPs were spherical. When more *Z. zerumbet* extracts were added, more spherical nanoparticles were formed. The hydrodynamic size changed slightly along with time, and the average size was approximately 170 nm. Capping of *Z. zerumbet* extract on the surface of gold nanoparticles was confirmed by Fourier transform infrared spectroscopy (FTIR). In general, phenolic compounds or flavonoid compounds were considered to be the reducing agent. However, zerumbone was identified as the reducing agent in this study. The resulting oxidized products were characterized by high-performance liquid chromatography-mass spectrometry (HPLC-MS). As a result, the solvent was proven to be involved in nanoparticle synthesis. Overall, Z zerumbet@Au NPs showed great potential to be used in cosmetic- or biomedicine-related fields.

1. Introduction

Many nanoparticle-related studies have been focused on the synthesis of nanoparticles. Gold nanoparticles are the most studied nanometal because they have unique optical, physical, and catalytic properties. In addition, the biocompatibility of gold nanoparticles enables them to have a wide range of applications in biomedicine- and biosensing-related fields [1–5]. Gold nanoparticles are easily modified by attaching nucleic acids, proteins, peptides, and organic compounds. Therefore, they are used as drug carriers and imaging reagents. Gold nanoparticles can also be used in cosmetics- and biomedicine-related fields [6–8].

When synthesizing gold nanoparticles, both reducing and capping agents are required to produce gold atoms and keep nanoparticles stable in solutions. Sodium borohydride, hydrazine, and surfactants are usually used in the synthesis of gold nanoparticles. Those synthetic reactions require inputted energy. If residual toxic chemicals are not completely removed, the entire biological system may be jeopardized. Therefore, the one-pot gold nanoparticle synthesis with plant extracts is an easy and eco-friendly method to avoid harmful chemicals adsorbed on the surface of nanomaterials [9–13]. The plant extract-capped gold nanoparticles provide better properties than chemically synthesized gold nanoparticles [12]. Biologically fabricated monometallic gold nanoparticles are considered to be a nanoantioxidant [14]. Studies showed that nanoantioxidants were better than natural antioxidants in radical scavenging and quenching capacities as the development of nanotechnology [8].

Z. zerumbet which is close to ginger has broad applications in herbal medicine such as relieving inflammation symptoms. In *Z. zerumbet,* zerumbone is the major active ingredient, and it has anti-inflammatory and anticancer activities [15–18]. Studies showed that the reducing and capping agents of gold nanoparticle synthesis with plant extracts were nontoxic phytochemicals [19, 20]. Although

the extract of *Z. zerumbet* had been used in silver nanoparticle synthesis [13], the reducing agent was not identified. On the other hand, green synthesis studies usually focus on nanoparticles. Synthesized compounds had not been identified. In fact, compounds formed and adsorbed on the gold nanoparticle surface with *Z. zerumbet* extracts (*Z. zerumbet*@Au NPs). Identification of those compounds will enhance the synthesis process for providing safer nanomaterials.

In this study, gold nanoparticles were first synthesized by a sustainable one-pot method with the aqueous extract of *Zingiber zerumbet* rhizome at room temperature. The morphology of *Z. zerumbet*@Au NPs was examined using a transmission electron microscope (TEM). The reductants in Z. zerumbet extract were identified by high-performance liquid chromatography (HPLC). Then, the resulting oxidized products were characterized by mass spectroscopy (MS). The surface coverage of synthesized gold nanoparticles was investigated by Fourier transform infrared spectroscopy (FTIR).

2. Material and Chemicals

2.1. Materials and Reagents. The rhizome of *Z. zerumbet* was bought from the local market in Taiwan. Chloroauric acid ($HAuCl_4{\cdot}3H_2O$) was purchased from Sigma-Aldrich Corporation (St. Louis, MO, USA). Methanol and acetonitrile (HPLC grade) were purchased from Mallinckrodt Baker Inc. (Phillipsburg, NJ, USA).

2.2. Sample Preparation. The rhizome of *Z. zerumbet* was washed thoroughly and then air-dried before extraction. *Z. zerumbet* rhizome was pulverized in methanol. For one gram of *Z. zerumbet* rhizome, 5 mL of methanol was used in each extraction. The rhizome of *Z. zerumbet* was extracted twice with methanol to achieve complete extraction. After collecting the extract, excess methanol was removed by using a rotary evaporator. After removing excess methanol, the residual extract was lyophilized. The dry extract was stored at −20°C for further experiments.

A stock aqueous extract was prepared by dissolving 0.2 gram of the dry *Z. zerumbet* extract in 10 mL of deionized water. The concentration of zerumbone in the solution was determined to be 1.36 mg/mL by HPLC. To synthesize gold nanoparticles, various volumes of the stock aqueous *Z. zerumbet* extract were added into 5 mL of the chloroauric acid solution (1 mM). The added volumes of stock aqueous *Z. zerumbet* extract were 0.125, 0.25, 0.5, 1.0, and 2.0 mL, respectively. The mixtures of *Z. zerumbet*@Au NPs were kept in the dark at room temperature during the reaction process.

2.3. Characterization of Z. zerumbet@Au NPs. *Z. zerumbet*@Au NPs were characterized by UV-visible spectroscopy (Jusco V-630 UV-VIS spectrophotometer, Tokyo, Japan). The morphology of *Z. zerumbet*@Au NPs was examined using a transmission electron microscope (TEM, JEM-2010, JEOL Ltd., Tokyo, Japan) equipped with a field-emission gun. The acceleration voltage was set to be 100 kV. To prepare samples for TEM analysis, the solution containing *Z. zerumbet*@Au NPs was centrifuged to remove residual reagent. After centrifugation, gold nanoparticles were resuspended with deionized water. Exactly 5 μL of purified gold nanoparticles was cast on a copper grid, then air-dried, and stored in a desiccator before TEM analysis. The hydrodynamic size of *Z. zerumbet*@Au NPs was measured with a Malvern Zetasizer Nano ZS instrument (Malvern Instrument LTD, Worcestershire, UK) at 25°C. Purified *Z. zerumbet*@Au NPs were resuspended in deionized water. The dispersant refractive index, viscosity, and dielectric constant were 1.33, 0.89 cps, and 78.5, respectively.

FT-IR spectroscopy was used to examine capping agents adsorbed on gold nanoparticles. Purified *Z. zerumbet*@Au NPs were dried before FT-IR analysis. The spectra of dry gold nanoparticles and plant extract were obtained using a Perkin–Elmer FT-IR spectrometer (Spectrum One, Waltham, MA, USA). Spectra of samples were recorded in the range of 400 to 4,000 cm^{-1} with a resolution of 4 cm^{-1}.

2.4. HPLC Analysis of Z. zerumbet Extract. *Z. zerumbet* extract and zerumbone standard solution were analyzed before and after gold nanoparticles synthesis by using a Perkin–Elmer HPLC instrument (250 LC Systems, Waltham, MA, USA) equipped with a 150 × 4.6 mm i.d. C18 column (ODS Hypersil, Thermo Fisher Scientific Inc., Waltham, MA, USA). The mobile phase was a mixture of acetonitrile and deionized water. The elution gradient was as follows: initial acetonitrile composition was set to 10%, increased to 90% in 30 minutes, and held at 90% for 5 minutes. The wavelength was set at 250 nm. When nanoparticle synthesis was completed, the reaction mixture was centrifuged with a centrifugal force of 9,870 G for 10 minutes. The supernatant which contained the residual *Z. zerumbet* extract or zerumbone solution was collected for HPLC analysis. All samples were passed through a 0.45 μm syringe filter before HPLC analysis.

The residual zerumbone solution was analyzed by using a Hitachi L7100 LC system coupled with a Finnigan LCQ Advantage electronspray ion-trap mass spectrometer (Thermal, San Jose, CA, USA) to identify obtained products after gold nanoparticle synthesis. The following parameters were set for mass analysis: the sheath gas flow rates and auxiliary gas flow rate were set at 35 and 10 arb, respectively. The ion spray voltage was 4.0 kV, and the capillary temperature was 230°C. Selected products were further subjected to collision-induced dissociation (CID) analysis to obtain the associated fragmentation spectra. All data were acquired in positive mode.

3. Results and Discussion

3.1. Synthesis of Z. zerumbet@Au NPs. After adding the aqueous *Z. zerumbet* extract to the chloroauric acid solution, UV-visible spectroscopy was used to monitor gold nanoparticle formation. The UV-visible spectra of synthesized gold nanoparticles are shown in Figure 1. The maximum absorption (λ_{max}) was around 550 nm because of the localized surface plasmon resonance of gold nanoparticles. As shown in Figure 1(a), gold nanoparticles started to form after one and half hours while the corresponding λ_{max} was

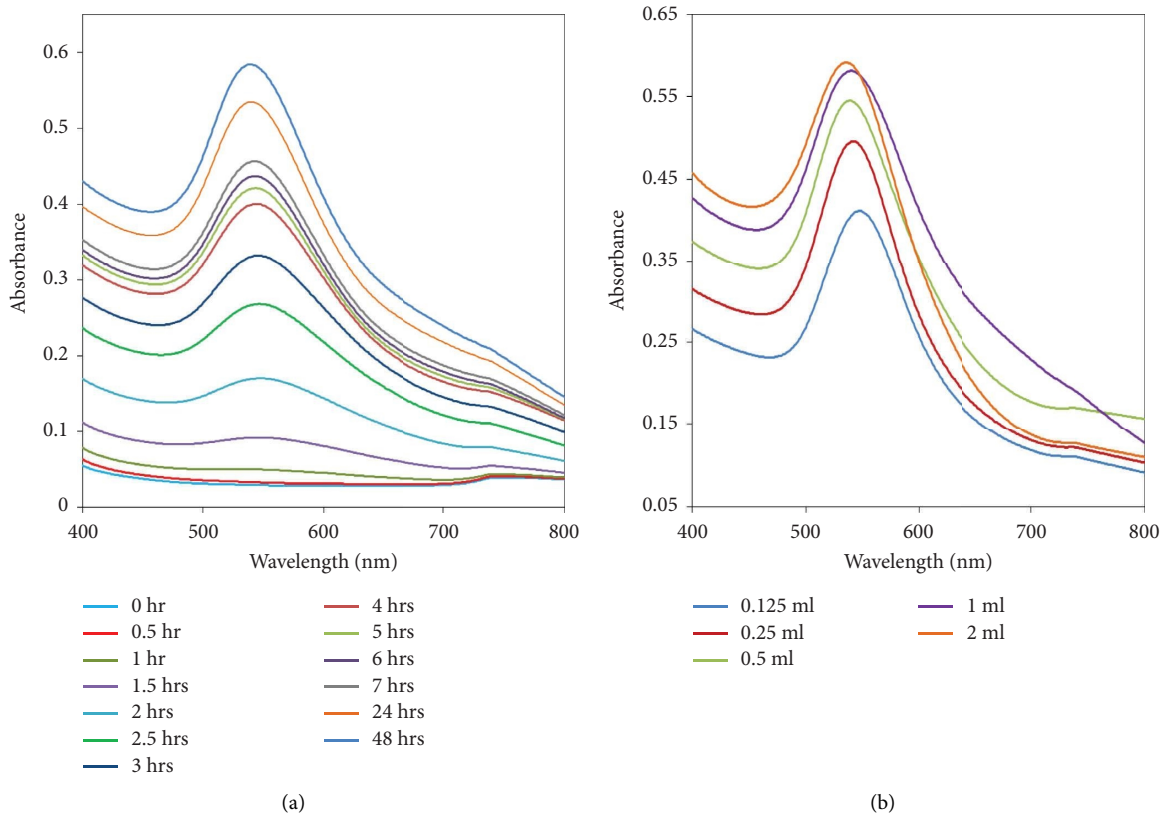

Figure 1: UV-visible spectra of *Z. zerumbet*@Au NPs. (a) One mL of *Z. zerumbet* extract was added to 5 mL of chloroauric acid solution. (b) Various volumes of *Z. zerumbet* extract were added to 5 mL of chloroauric acid solution. The spectra were recorded after 48 hours of addition.

around 548 nm. Since the synthesis was performed at room temperature, the reaction rate was slower than that of the Turkevich method with hot chloroauric acid. The λ_{max} is decreased to around 539 nm after 48 hours of reaction. Although the reaction rate was slower, no extra energy was required. During the synthesis process, smaller gold nanoparticles formed, and the λ_{max} changed from 548 to 539 nm. Based on Figure 1(b), the size of gold nanoparticles was affected by the amount of *Z. zerumbet* extract. When more *Z. zerumbet* extract was added, the gold nanoparticle size decreased. For example, when extracts increased from 0.125 to 2.0 mL, the λ_{max} of gold nanoparticles decreased from 550 to 536 nm (Figure 1(b)).

3.2. Characterization of Z. zerumbet@Au NPs by TEM and FT-IR. The morphology of gold nanoparticles was examined by TEM. Figure 2 shows the TEM images of *Z. zerumbet*@Au NPs. Based on Figure 2, gold nanoparticles were polymorphic including spheres, triangles, bars, and irregular shapes. Most of the gold nanoparticles were spherical. However, some nanoparticles looked like icosahedrons and hexagons. The percentages of spheres, triangles, and bars are summarized in Table 1.

The percentage of spherical gold nanoparticles was greater than 80% in all cases. Based on Table 1, when more *Z. zerumbet* extract was added, more spherical nanoparticles were formed. Because more than 80% of nanoparticles were spherical, only spherical nanoparticles were counted when calculating particle diameter. When the volume ratio (*Z. zerumbet* extract/$HAuCl_4$ solution) increased, the average size of gold nanoparticles decreased (Table 1) and the spherical particle size distribution range decreased (Figure 2). As a result, adding more plant extracts reduced the gold nanoparticle size. $HAuCl_4$ molecules were reduced to gold nanoparticles when adding more plant extracts. Once gold nanoparticles are formed, compounds originating from plant extract are attached to the surface of gold nanoparticles as capping agents. Thus, they kept gold nanoparticles from aggregation. When the volume ratio was high, more gold ions were reduced, and then, more compounds were able to attach on the gold nanoparticle surface. That resulted in the formation of small gold nanoparticles and size distribution.

The hydrodynamic size of selective *Z. zerumbet*@Au NPs at various time intervals was measured. The results showed that the particle size changed slightly along with time (Table 2).

The determination of hydrodynamic size considered the hydration layer, capping agents, and other compounds that may stabilize nanoparticles. Therefore, the hydrodynamic size is usually larger than the size observed in TEM images. According to Table 2, the hydrodynamic size changed slightly along with time, and the average size was approximately 170 nm.

The functional groups of capping agents on the gold nanoparticle surface were examined using IR spectroscopy. Figure 3 shows the IR spectra of *Z. zerumbet* extract and

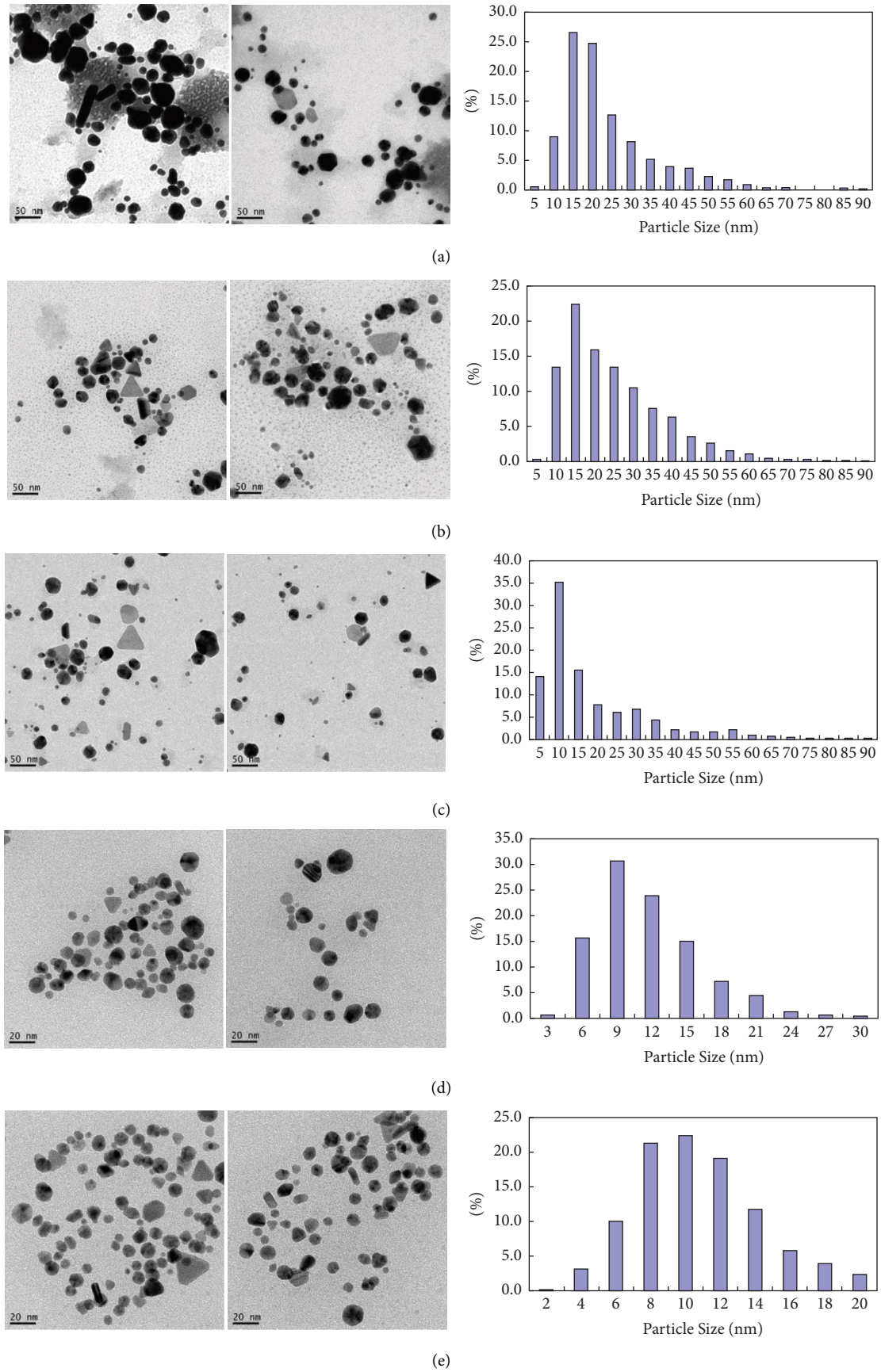

Figure 2: Morphology and particle size distribution of synthesized gold nanoparticles. The volume ratios ($V_{ext.}/V_{HAuCl_4}$) in (a–e) were 0.025, 0.05, 0.1, 0.2, and 0.4, respectively.

Table 1: The average size and shape of synthesized gold nanoparticles.

Volume ratios $V_{ext.}/V_{HAuCl_4}$	Average particle size (nm)	Shape (%)			
		Spheres	Triangles	Bars	Others*
0.025	21.3 ± 12.2	82.8	3.1	1.2	13.0
0.05	22.5 ± 13.0	88.5	5.4	3.3	2.8
0.1	16.0 ± 14.2	91.2	4.2	1.9	2.8
0.2	10.2 ± 4.6	89.6	7.6	2.0	0.8
0.4	9.3 ± 3.4	90.8	5.1	3.1	0.9

*Others included icosahedrons and hexagons.

Table 2: Hydrodynamic size of selective *Z. zerumbet*@Au NPs.

	Time (days)				
	1	2	9	16	23
Hydrodynamic size (nm)	170.80 ± 6.14	145.25 ± 3.99	177.38 ± 6.87	140.80 ± 3.50	198.93 ± 3.21

The volume ratio (*Z. zerumbet* extract/$HAuCl_4$ solution) was 0.05.

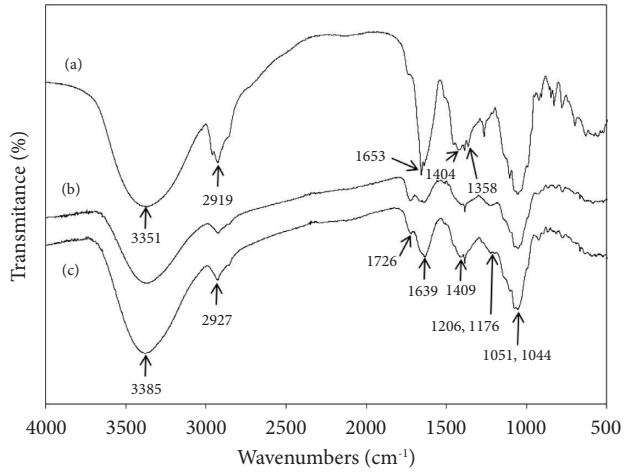

Figure 3: IR spectra of *Z. zerumbet* extract and *Z. zerumbet*@Au NPs. (a) *Z. zerumbet* extract. (b and c) *Z. zerumbet*@Au NPs with the volume ratios (*Z. zerumbet* extract/$HAuCl_4$ solution) of 0.2 and 0.4, respectively.

extract-capped gold nanoparticles. Panel (A) was the IR spectrum of *Z. zerumbet* extract. The panels (B) and (C) were IR spectra of gold nanoparticles capped with *Z. zerumbet* extract with volume ratios (*Z. zerumbet* extract/$HAuCl_4$ solution) of 0.2 and 0.4, respectively. Based on Figure 3, the IR spectra of *Z. zerumbet*@Au NPs were similar to that of *Z. zerumbet* extract. Similar IR profiles indicated that the capping agents on the gold nanoparticle surface originated from *Z. zerumbet* extract. More *Z. zerumbet* extracts were added indicating higher plant extract concentration on the gold nanoparticle surface. Thus, the IR signal intensity increased.

The signal that appeared at 3385 cm^{-1} corresponded to the stretching vibration of hydroxyl groups that originated from various compounds such as polyphenols, flavonoids, and saccharides. To obtain stable gold nanoparticles, various compounds in plant extracts were attached to the surface of nanoparticles via amino, carbonyl, or hydroxyl groups after nucleation. When compared with the signals of *Z. zerumbet* extract, the position slightly shifted from 3351 to 3385 cm^{-1}. This change indicated the attaching of capping agents via hydroxyl groups. In the *Z. zerumbet* extract spectrum, peaks appeared at 1653, 1404, and 1358 cm^{-1} were attributed to the absorption of zerumbone. Zerumbone was the major component in *Z. zerumbet* extract. These values agreed with those reported in literature. Literature reported that the α, β-unsaturated carbonyl group of zerumbone and its derivatives gave the stretching vibration signal at 1655 cm^{-1}, whereas the germinal dimethyl groups gave the starching signal at 1385 and 1356 cm^{-1} [21]. The corresponding signals of 1639 and 1409 cm^{-1} were observed with the presence of gold nanoparticles but the intensity decreased. The absorption at 1726 cm^{-1} became prominent. This signal may be originated from the carbonyl stretching of compounds with functional groups such as aldehyde or ketone. Because zerumbone was consumed during synthesis, it may serve as the reducing or capping agent (based on HPLC results). As a result, the signal of 1726 cm^{-1} from other compounds became visible due to the reduction of zerumbone concentration. Other absorptions at 2927 and 1051 cm^{-1} could

be assigned to C-H and C-O stretching, respectively. Detailed IR signal assignments including all possible functional groups are shown in Table 3. Because IR profiles of *Z. zerumbet* extract and *Z. zerumbet*@Au NPs were similar, compounds in *Z. zerumbet* extract served as the capping agents.

3.3. HPLC Analysis of Z. zerumbet Extract. Velmurugan et al. used the *Zingiber officinale* root extract to synthesize gold and silver nanoparticles [22]. They speculated that water-soluble ingredients such as ascorbic and oxalic acids were the reductants. However, no further analysis was provided [22]. In this study, HPLC was used to investigate the specific compound in *Z. zerumbet* extract which was involved in the gold nanoparticle formation. *Z. zerumbet* extracts were analyzed by HPLC before and after gold nanoparticle formation. The analytical results are shown in Figure 4. The upper and lower panels of Figure 4(a) were HPLC chromatograms of *Z. zerumbet* extract and the corresponding residue after nanoparticle synthesis, respectively. The peak at 26.4 min was zerumbone. The HPLC chromatogram of residual *Z. zerumbet* extract did not show the corresponding peak at 26.4 min. However, two peaks appeared at 15.5 and 17.2 min. These changes in *Z. zerumbet* extract composition indicated that zerumbone participated in gold nanoparticle formation. Zerumbone was the reducing agent in gold nanoparticle synthesis.

To confirm that zerumbone served as reducing and capping agents, the zerumbone standard was used to synthesize gold nanoparticles and the residual solution was analyzed by HPLC. Twenty-four hours after adding the zerumbone standard, gold nanoparticles were formed and the solution turned purplish. Zerumbone and resulting products were the capping agents since only the zerumbone standard was added. Because these gold nanoparticles easily precipitated, they were not as stable as *Z. zerumbet*@Au NPs. The stability of *Z. zerumbet*@Au NPs was attributed to plant phytochemicals such as flavonoids, polyphenols, terpenoids, and other compounds including proteins and amino acids [19, 20]. These compounds served as capping and reducing agents. Literature also revealed the presence of polyphenols and flavonoids in *Z. zerumbet* [13, 23]. When *Z. zerumbet* extract was used in synthesis, capping agents were assorted to produce stable gold nanoparticles.

The upper panel of Figure 4(b) was the HPLC chromatogram of the residual zerumbone solution after synthesis. Similar to the plant extract, zerumbone was used up, and new peaks (1, 2, and 3) appeared at around 16.0, 17.2, and 22.5 min after synthesis. The disappearance of the zerumbone peak indicated that zerumbone was used up. Zerumbone was oxidized to reduce chloroauric acid to gold. In addition, the reducing power of zerumbone was compared with that of sodium citrate by synthesizing gold nanoparticles in the presence of zerumbone and sodium citrate. The lower panel of Figure 4(b) was the HPLC chromatogram of the residual reaction mixture. In the presence of sodium citrate, the zerumbone was not completely consumed and the oxidized products were less.

Table 3: IR absorption of *Z. zerumbet* extract and *Z. zerumbet*@Au NPs.

Absorption frequency (cm^{-1})	Origination of IR absorption
3385 (3351)	-OH stretching of polyphenols or flavonoids -NH stretching of amide
2927 (2919)	-CH stretching of methylene and methyl groups
1726	
1639 (1653)	Carbonyl stretching of -C=C-CO-C=C- group of zerumbone Carbonyl stretching of amide I band
1409 (1404/1358)	Germinal dimethyl stretching of zerumbone Aromatic C=C ring stretching
1051/1044	C-O stretching of alcohol

According to HPLC results, zerumbone in *Z. zerumbet* extract was the reducing agents in gold nanoparticle synthesis. When sodium citrate and zerumbone were present, both compounds reduced the chloroauric acid and then produced gold nanoparticles.

The oxidation products resulting from the zerumbone in nanoparticle synthesis were identified by mass spectroscopy. Table 4 shows the mass of three major products (compounds 1, 2, and 3) and their parent collision-induced fragments. Because the detecting wavelength was 250 nm in HPLC analysis, all compounds observed should have the same conjugation as zerumbone. According to the retention time, compounds 1, 2, and 3 all had higher polarity than zerumbone. The increase in mass indicated the addition of an oxygen atom to the structure. Because epoxide has a higher ring strain, hydroxylation is more likely to occur. The structures of oxidized products were assigned tentatively according to the collision-induced fragments and their stability. These oxidized products were either hydroxylated or methoxylated depending on whether methanol was present during synthesis. Compared with the zerumbone, the mass of compounds 1 and 2 increased by 16 mass units, and their fragmentation patterns were the same (data were not shown). Therefore, compounds 1 and 2 had the same skeletal structure with an additional hydroxyl group attached at different positions (Table 4). The orientation of the hydroxyl group could not be distinguished by mass spectrometry. Based on the molecular weight difference and collision fragments, compound 3 had an additional methoxy group attached either at the C4 or the C5 position (Table 4). Because the zerumbone used in nanoparticle synthesis was dissolved in methanol, the methoxy group could originate from the solvent. However, the aqueous *Z. zerumbet* extract was used in the synthesis. Thus, compound 3 was not observed in the HPLC chromatogram of residual plant extract. As a result, it is clearly indicated the participation of solvent during nanoparticle synthesis. The reaction mechanism of gold nanoparticle synthesis using plant extracts was not clear. In general, phenolic compounds and flavonoids were thought to be the reductants and capping agents [20, 24–26]. Ramzan et al. used

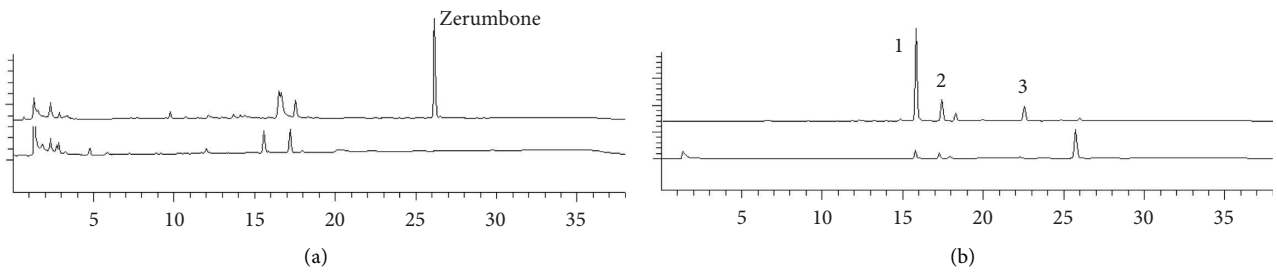

Figure 4: (a) HPLC chromatograms of *Z. zerumbet* extract and reaction residue. The upper panel is the HPLC chromatogram of *Z. zerumbet* extract, whereas the lower panel is that of residual *Z. zerumbet* extract after gold nanoparticle formation. (b) The upper panel is the HPLC chromatogram of residual zerumbone solution after gold nanoparticle formation, whereas the lower panel is that of residual zerumbone solution in the presence of sodium citrate.

Table 4: The chemical structure of oxidized products and the parent collision-induced fragments.

Compound	Retention time (min)	Molecule mass	m/z value*	Chemical structure
Zerumbone	26.1	218	201.2	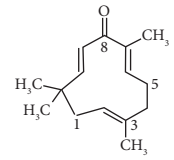
1	16.0	234	217.13	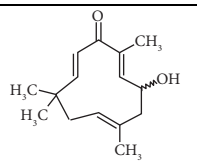
2	17.2	234	217.07	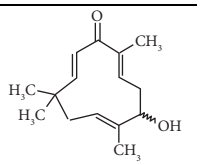
3	22.5	248	217.08	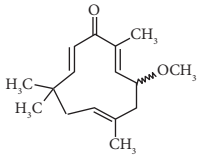

*The parent collision-induced fragment.

standard phytochemical tests to assess alkaloids, phenolic compounds, and flavonoids in *Z. zerumbet* extract [13]. They concluded that these phytochemicals were responsible for AgNP reduction and capping based on the qualitative results. However, the HPLC results of this study showed that zerumbone, not phenolic compounds or flavonoid compounds, was the reducing agent for gold nanoparticle formation.

4. Conclusions

Z. zerumbet extract-mediated green production of gold nanoparticles was established in this study. Based on the UV spectroscopy and TEM results, most *Z. zerumbet*@Au NPs were spherical. The hydrodynamic size changed slightly along with time, and the average size was approximately 170 nm. However, the correlation between size and shape requires more studies to provide uniform nanoparticles. Based on the HPLC and MS results, zerumbone served as the reducing agent during the gold nanoparticle synthesis. Zerumbone was oxidized and then mixed with other compounds in *Z. zerumbet* extract to be the capping agent to stabilize gold nanoparticles. The functional groups of capping agents on the gold nanoparticle surface were determined by FT-IR. The solvent was proven to be involved in nanoparticle synthesis. The oxidized compounds were formed and adsorbed on the gold nanoparticle surface. The solvent effect needs to be considered for providing safer nanoparticles with less toxicity.

Data Availability

The data supporting the current study are available from the corresponding author upon request.

Conflicts of Interest

The authors declare that they have no conflicts of interest.

References

[1] E. C. Dreaden, A. M. Alkilany, X. Huang, C. J. Murphy, and M. A. El-Sayed, "The golden age: gold nanoparticles for biomedicine," *Chemical Society Reviews*, vol. 41, no. 7, pp. 2740–2779, 2012.

[2] X. Yang, M. Yang, B. Pang, M. Vara, and Y. Xia, "Gold nanomaterials at work in biomedicine," *Chemical Reviews*, vol. 115, no. 19, pp. 10410–10488, 2015.

[3] Z. Hua, T. Yu, D. Liu, and Y. Xianyu, "Recent advances in gold nanoparticles-based biosensors for food safety detection," *Biosensors and Bioelectronics*, vol. 179, Article ID 113076, 2021.

[4] J. A. Buledi, S. Amin, S. I. Haider, M. I. Bhanger, and A. R. Solangi, "A review on detection of heavy metals from aqueous media using nanomaterial-based sensors," *Environmental Science and Pollution Research*, vol. 28, no. 42, pp. 58994–59002, 2021.

[5] W. B. Tseng, M. M. Hsieh, C. H. Chen, T. C. Chiu, and W. L. Tseng, "Functionalized gold nanoparticles for sensing of pesticides: a review," *Journal of Food and Drug Analysis*, vol. 28, no. 4, pp. 521–538, 2020.

[6] E. B. Souto, A. R. Fernandes, C. Martins-Gomes et al., "Nanomaterials for skin delivery of cosmeceuticals and pharmaceuticals," *Applied Sciences*, vol. 10, no. 5, p. 1594, 2020.

[7] E. Bellu, S. Medici, D. Coradduzza, S. Cruciani, E. Amler, and M. Maioli, "Nanomaterials in skin regeneration and rejuvenation," *International Journal of Molecular Sciences*, vol. 22, no. 13, p. 7095, 2021.

[8] L. Liu, W. Zhao, Q. Ma et al., "Functional nano-systems for transdermal drug delivery and skin therapy," *Nanoscale Advances*, vol. 5, no. 6, pp. 1527–1558, 2023.

[9] A. Baran, C. Keskin, M. F. Baran et al., "Ecofriendly synthesis of silver nanoparticles using Ananas comosus fruit peels: anticancer and antimicrobial activities," *Bioinorganic Chemistry and Applications*, vol. 2021, Article ID 2058149, 8 pages, 2021.

[10] A. Baran, M. F. Baran, C. Keskin et al., "Ecofriendly/rapid synthesis of silver nanoparticles using extract of waste parts of artichoke (Cynara scolymus L.) and evaluation of their cytotoxic and antibacterial activities," *Journal of Nanomaterials*, vol. 2021, Article ID 2270472, 10 pages, 2021.

[11] J. Qiao and L. Qi, "Recent progress in plant-gold nanoparticles fabrication methods and bio-applications," *Talanta*, vol. 223, no. 2, Article ID 121396, 2021.

[12] U. M. Muddapur, S. Alshehri, M. M. Ghoneim et al., "Plant-based synthesis of gold nanoparticles and theranostic applications: a review," *Molecules*, vol. 27, no. 4, p. 1391, 2022.

[13] M. Ramzan, M. I. Karobari, A. Heboyan et al., "Synthesis of silver nanoparticles from extracts of wild ginger (Zingiber zerumbet) with antibacterial activity against selective multidrug resistant oral bacteria," *Molecules*, vol. 27, no. 6, p. 2007, 2022.

[14] B. Omran and K. H. Baek, "Nanoantioxidants: pioneer types, advantages, limitations, and future insights," *Molecules*, vol. 26, no. 22, p. 7031, 2021.

[15] J. W. Tan, D. A. Israf, and C. L. Tham, "Major bioactive compounds in essential oils extracted from the rhizomes of Zingiber zerumbet (L) Smith: a mini-review on the anti-allergic and immunomodulatory properties," *Frontiers in Pharmacology*, vol. 9, p. 652, 2018.

[16] A. Murakami, R. Hayashi, T. Takana, K. H. Kwon, H. Ohigashi, and R. Safitri, "Suppression of dextran sodium sulfate-induced colitis in mice by zerumbone, a subtropical ginger sesquiterpene, and nimesulide: separately and in combination," *Biochemical Pharmacology*, vol. 66, no. 7, pp. 1253–1261, 2003.

[17] M. R. Sulaiman, E. K. Perimal, M. N. Akhtar et al., "Anti-inflammatory effect of zerumbone on acute and chronic inflammation models in mice," *Fitoterapia*, vol. 81, no. 7, pp. 855–858, 2010.

[18] K. Kalantari, M. Moniri, A. Boroumand Moghaddam et al., "A review of the biomedical applications of zerumbone and the techniques for its extraction from ginger rhizomes," *Molecules*, vol. 22, no. 10, p. 1645, 2017.

[19] V. Kharissova, H. R. Dias, B. I. Kharisov, B. O. Pérez, and V. M. J. Pérez, "The greener synthesis of nanoparticles," *Trends in Biotechnology*, vol. 31, no. 4, pp. 240–248, 2013.

[20] M. Ovais, A. T. Khalil, N. U. Islam et al., "Role of plant phytochemicals and microbial enzymes in biosynthesis of metallic nanoparticles," *Applied Microbiology and Biotechnology*, vol. 102, no. 16, pp. 6799–6814, 2018.

[21] E. E. M. Eid, A. B. Abdul, F. E. O. Suliman, M. A. Sukari, A. Rasedee, and S. S. Fatah, "Characterization of the inclusion complex of zerumbone with hydroxypropyl-β-cyclodextrin," *Carbohydrate Polymers*, vol. 83, no. 4, pp. 1707–1714, 2011.

[22] P. Velmurugan, K. Anbalagan, M. Manosathyadevan et al., "Green synthesis of silver and gold nanoparticles using Zingiber officinale root extract and antibacterial activity of silver nanoparticles against food pathogens," *Bioprocess and Biosystems Engineering*, vol. 37, no. 10, pp. 1935–1943, 2014.

[23] C. B. Singh, K. Nongalleima, S. Brojendrosingh, S. Ningombam, N. Lokendrajit, and L. W. Singh, "Biological and chemical properties of Zingiber zerumbet Smith: a review," *Phytochemistry Reviews*, vol. 11, no. 1, pp. 113–125, 2012.

[24] M. Teimouri, F. Khosravi-Nejad, F. Attar et al., "Gold nanoparticles fabrication by plant extracts: synthesis, characterization, degradation of 4-nitrophenol from industrial wastewater, and insecticidal activity-A review," *Journal of Cleaner Production*, vol. 184, pp. 740–753, 2018.

[25] M. S. Mehata, "Green route synthesis of silver nanoparticles using plants/ginger extracts with enhanced surface plasmon resonance and degradation of textile dye," *Materials Science and Engineering: B*, vol. 273, Article ID 115418, 2021.

[26] G. Barman, S. Maiti, and J. K. Laha, "Bio-fabrication of gold nanoparticles using aqueous extract of red tomato and its use as a colorimetric sensor," *Nanoscale Research Letters*, vol. 8, no. 1, p. 181, 2013.